

СООБЩЕНИЯ
ОБЪЕДИНЕННОГО
ИНСТИТУТА
ЯДЕРНЫХ
ИССЛЕДОВАНИЙ

Дубна

E13-97-355

P.Antich¹, R.Parkey¹, E.Tsyganov¹, A.Zinchenko

A SUPERFIBER FOR POSITION
SENSITIVE DETECTORS

¹The University of Texas Southwestern Medical Center at Dallas, USA

«Суперфайбер» для позиционно-чувствительных детекторов

Сцинтилляционные волокна все чаще используются в науке и медицине при создании координатных систем с высокой точностью для регистрации заряженных частиц и фотонов. Однако низкая эффективность светосбора до сих пор является их главным недостатком.

Представлены результаты моделирования методом Монте Карло, иллюстрирующие особенности распространения света в круглых волокнах. Показано, что после некоторых изменений геометрии волокон эффективность светосбора в них может быть повышена до 20 % в одном направлении.

Работа выполнена в Лаборатории высоких энергий ОИЯИ.

Сообщение Объединенного института ядерных исследований. Дубна, 1997

A Superfiber for Position Sensitive Detectors

Scintillating fibers are being more and more used in science and medicine to provide precise coordinate measurement systems for elementary particles and x-ray detection. However, low light collection efficiency is still most limiting factor.

We present results of Monte Carlo calculations to illustrate some peculiarities of light collection in round fibers. According to our analyses, by certain modifications light collection in round scintillating and waveshifting fibers could be increased to about 20 % per direction.

The investigation has been performed at the Laboratory of High Energies, JINR.

1. Introduction

Scintillating and light guiding fibers are commonly used in science and medicine to detect positions of nuclear particles and x-rays [1]. Fast response, good position resolution, and the ability to form a complex geometry are among the most attractive features of fiber devices. A major deficiency of scintillating fibers is their limited light collection efficiency. In round fibers light collection efficiencies are typically ~3% and ~5% for single and double cladding layers, respectively[2].

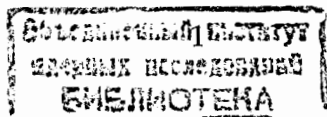
Light collection and transport in scintillating fibers rely on the process of internal reflection. At an optical interface, internal reflection occurs if the angle of incidence with respect to the surface normal is larger than a critical angle θ_c . At angles smaller than θ_c , light can be partially reflected or refracted. Snell's law describes the relation between the incident θ_1 and refracted θ_2 angles as

$$\frac{\sin(\theta_1)}{\sin(\theta_2)} = \frac{n_2}{n_1} \quad (1.1)$$

where n_1 and n_2 are the respective indices of refraction. The critical angle is obtained by setting $\sin(\theta_2)$ equal to 1. In the simple case of light emission on the axis of a round fiber, only that fraction emitted into an axial cone of angle $\pi/2 - \theta_c$ is captured. The remaining light eventually escapes through refraction. Based on these simple relations, we have made Monte Carlo calculations to investigate optimal configurations for light collection in round fibers.

2. Monte Carlo Model

Our aim was to evaluate the maximum possible gain in the light collection, which could be achieved in fibers. Our use of the Monte Carlo model is based solely on a geometric approach to light propagation processes. At the media boundary, the photon can be either reflected or refracted depending on the angle of incidence and ratio of media's refraction indices. The reflection coefficient can be varied and is assumed to be independent of the light wavelength and incident angle. Refraction indices were also supposed to be not depended on the light



wavelength. Other relevant phenomena, such as light tunneling through cladding layers, are not considered in this model.

We used fibers covered by a cladding layer about 20 μm thick. The refraction index of the plastic scintillator was taken to be 1.59 which corresponds to a polystyrene based scintillator, and that of the cladding was assumed to be 1.49 which corresponds to an acrylic. Internal reflection efficiency was assumed to be 100% at interior scintillator-cladding interfaces. To model leakage at the cladding-air interface, the reflection efficiency was varied (mechanical defects and surface contamination alter this value). In practice, an absorber layer external to the cladding layer is used sometimes, to eliminate the light leakage and optical cross-talk between the fibers.

For the Monte Carlo calculations, a mean of 50 photon source was chosen as a typical low level light signal. In plastic scintillators, where Compton scattering is the dominant x-ray interaction mode, 50 photons correspond to about 5 keV of recoil electron energy. A point source was used in the modeling. A Poisson distribution was used to generate the actual number of photons in the event. Photon directions were generated isotropically.

The light source was situated mid-way along the fiber length, the transaxial position was a variable parameter. Typical, fiber lengths were set at 1 m length and photons were counted at both ends of the fiber. Round and rectangular fiber profiles were tested. Typically, 1000 light flashes (events) were generated for each parameter set studied. To meet practical timing resolution limits, the time-of-flight was calculated for each photon and a 10 ns cut was applied. The number of reflections per photon was also evaluated.

3. Results and Discussion

Figure 1 presents the dependence of the light yield on the radial position of the light source for a 1 mm diameter single cladding fiber 2 m in length. The upper curve (open circles) represents the case for a 100% reflection efficiency at the cladding-to-air interface ($k_2 = 1$). The light yield is surprisingly high in contrast to the 3% experimental value previously mentioned. However, with the introduction of a slightly lower, but optimistic efficiency of $k_2 = 0.99$ (solid squares), the yield was decreased to more realistic values. Thus, even with a small optical

inefficiency at the outer cladding surface, multiple reflections will allow light in the cladding to escape. For the $k_2 = 0$ case (solid circles) the yield is not much different from the $k_2 = 0.99$. Therefore, in all of our calculations the efficiency at the outer cladding surface was set to zero.

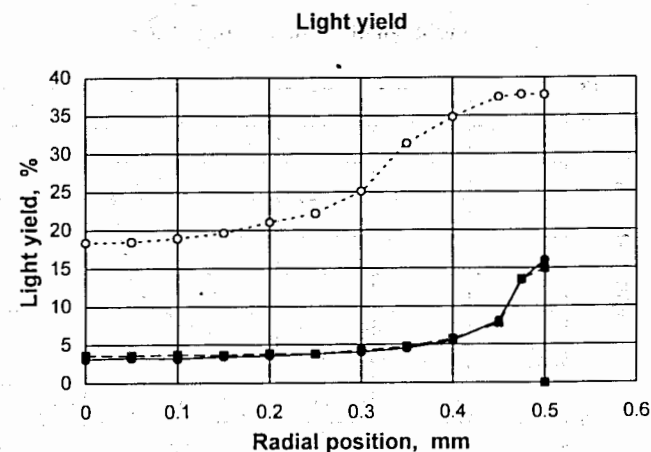


Figure 1. Light yield from one end of a fiber versus radial position of light source for round fibers (1 mm in diameter). Open circles - for the case when internal reflection efficiency at cladding-air boundary is 100%, square - 99%, and solid circles - 0%.

Figure 2 demonstrates the radial dependence of light collection in greater detail. Fig. 2a shows the one-ended light yield as a function of radial position. Fig. 2b and Fig. 2c show the photon distributions (summed from both fiber ends) for light sources located at the center and inner boundary of the fiber core, respectively. The light yield has a strong radial dependence, and can vary as much as a factor of 5 between the center and the edge. This effect is well known and is caused by a light guiding effect of the internal surface of the round fiber [4,5]. At the very proximity of the cylindrical surface, helical light trajectories are possible, and the available solid angle for internal reflection increases. Unfortunately, the light collection time will also increase, but this time still can be well within acceptable limits.

Figure 3 shows light yield dependence for a rectangular fiber, the source position was varied from the center out along a normal face. Not

surprisingly, the positional transaxial light yield dependence for rectangular fiber was found to be uniform. Although the light yield is relatively low, the flat response of the rectangular fiber geometries provides uniform energy deposition measurements.

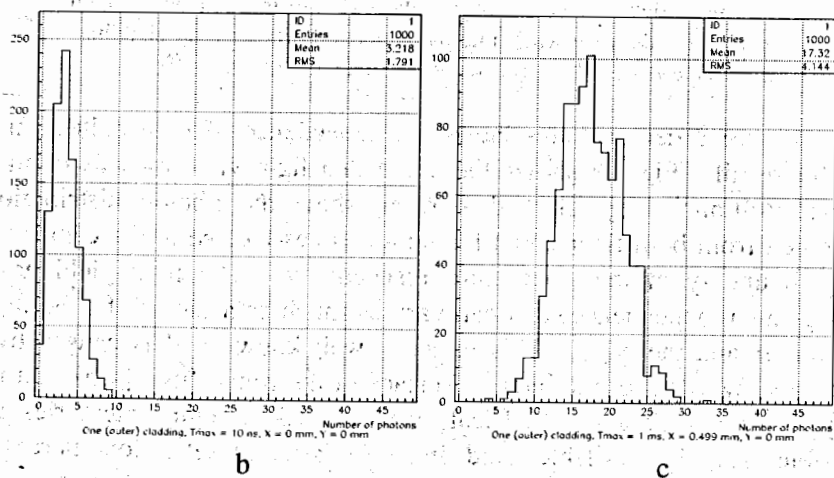
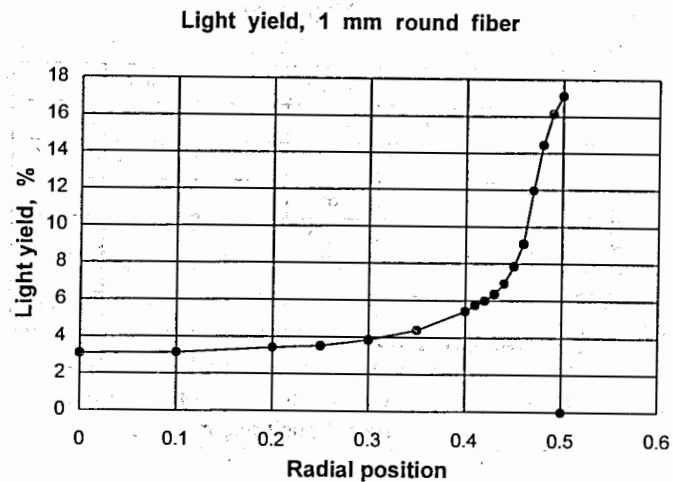


Fig. 2. Light collection in a round fiber versus radial position of a source: a - light yield, b - distribution of number of photons for a source position at center of fiber, c - the same for a source position at radius of 0.499 mm.

Light yield, square fiber 1 mm x 1 mm

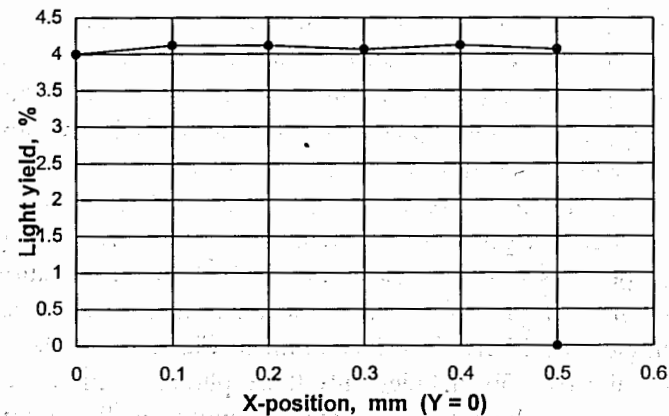


Figure 3. Light yield dependence versus source position for a square fiber.

Multilayer Round Fiber

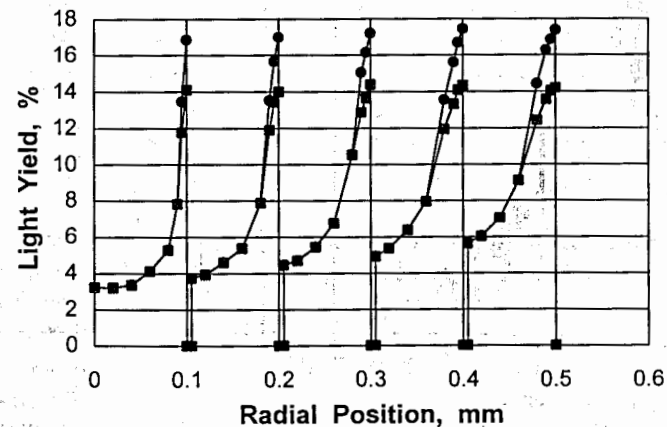


Figure 4. Light yield dependence in a round fiber interlayered with four additional cylindrical cladding layers. Round solid dots are for no photon travel time cut, and lower solid squares are for the photon travel time of 10 ns for 50 cm fiber length.

The results presented in Fig. 2a suggest a modification to traditional round fiber design. Light yields can be increased by introducing additional concentric layers of cladding in the fiber construction. We call this design a *Superfiber*. Figure 4 presents light yields for a fiber with four 5 μm thick interior cylindrical cladding layers in a 1 m long fiber. Solid dots are yield including all photon travel times, and the lower solid squares are for photons with a 10 ns time-of-flight cut applied. The potential for increased light yield using a *Superfiber* design is apparent.

To investigate the relative importance of delayed flight photons in the superfiber design, time-of-flight intervals were averaged for the surviving photons in each event. Figure 5 shows the resulting averaged time-of-flight histogram for a source located just inside the periphery of a 1 mm single clad fiber. The histogram in Fig. 5a includes all surviving photons while Fig. 5b includes only those photons with a travel time less than 10 ns. Since the results indicate that only a small fraction of the light actually travels *slow* (*i.e.*, those photons emitted perpendicular to the fiber axis), the influence of this *slow* fraction can be largely ignored.

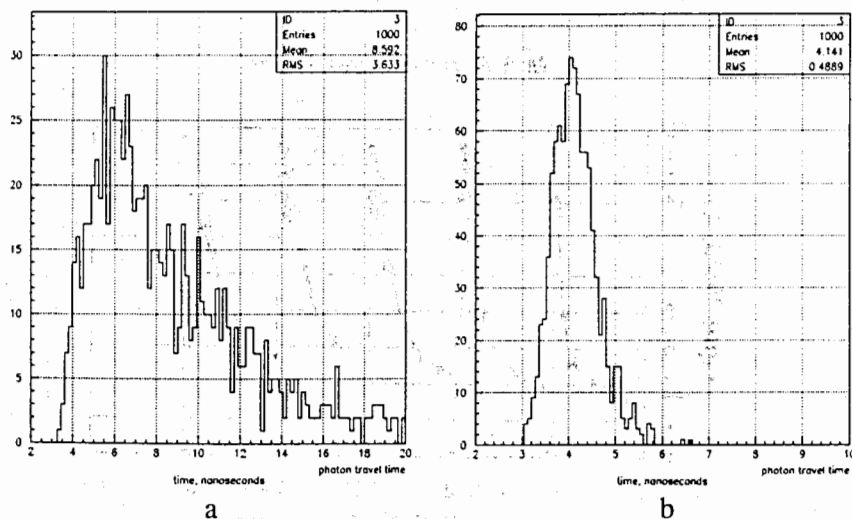


Figure 5. Distributions of time-of-flight intervals averaged over all surviving photons in an event for a radial position of 0.499 mm in a single cladding fiber. Figure 5a gives results with no time-of-flight cut, and Figure 5b shows results when the time-of-flight cut rejects all photons with a travel time $t > 10$ ns.

The results in Fig. 4 clearly show that the average light yield for the *Superfiber* design is significantly increased, despite the introduction of passive materials (intercladdings). To calculate the average light yield for an actual fiber we modelled a uniform transaxial light source distribution in such a fiber. The transaxial section was located at the midpoint of the fiber length. Figure 6 shows the distribution of the number of detected photons for the fiber design of Figure 4 with a 10 ns time-of-flight cut applied. The average light yield is increased to eight percent.

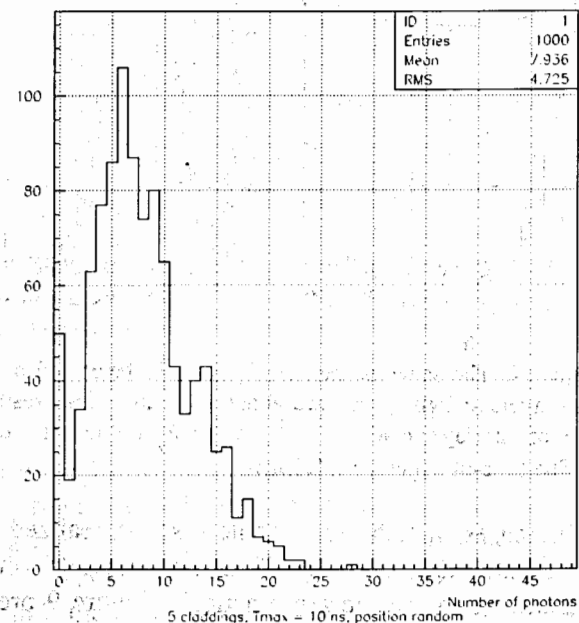


Figure 6. Distribution of the number of photons detected for the fiber design of Fig. 4. The average light yield is about 8%. The time-of-flight cut is 10 ns.

Light yields for 10-layer and 20-layer fiber designs with interlayer cladding thickness of 2 μm and 1 μm , respectively, were also modelled. The results presented in Figure 7 indicate the fraction of events in the non-scintillating passive material in either of the two cases was only about 3%. This percentage would be further decreased for Compton recoil energies in excess of about 10 keV, when an electron travels out from an intercladding layer. The light yields are increased to $\sim 10\%$ for the 10-

layer and to ~12% for the 20-layer fiber. For comparison, Figure 8 shows the average light yield for a conventional one-cladding fiber.

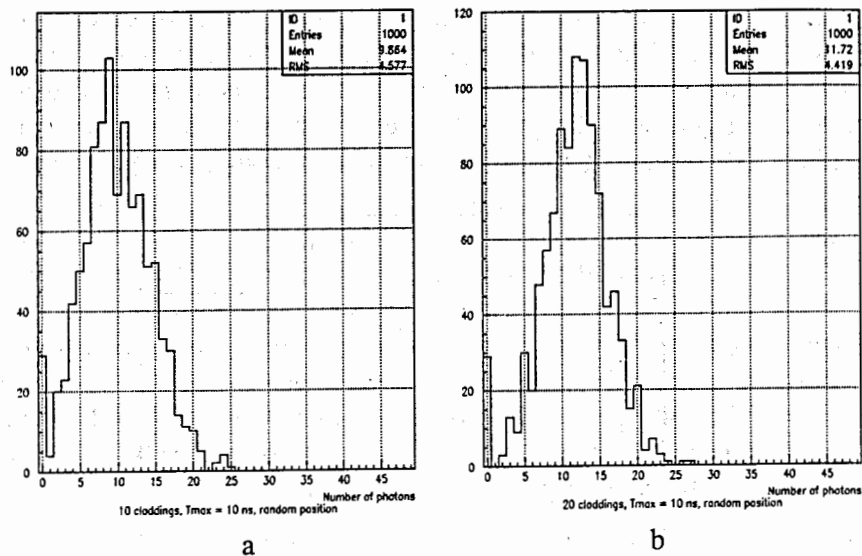


Figure 7. The same as for Fig. 6 for a) 10-layer and b) 20-layer fiber. The average light yields are about 10% and 12%, respectively. Thickness of interlayer cladding is 2 μm in the case a) and 1 μm in the case b). The time-of-flight cut is 10 ns.

Further increases in light yield could also be realized by potential improvements of cladding material. Cladding materials with refractive indices lower than that for acrylic are practical. Figure 9 presents a case for a 20-layer fiber interlayered with a material having a refractive index of 1.39. Here a yield of ~18% is achieved. Figure 10 presents the distribution of the average number of reflections for this *high-yield* fiber. The number of multiple reflections is large for a *high-yield* fiber (in this case about 7000) and clearly shows the necessity to provide a high-efficiency for internal reflection. Surface uniformity is also a critical factor; however, we believe that present day technologies can meet this requirement.

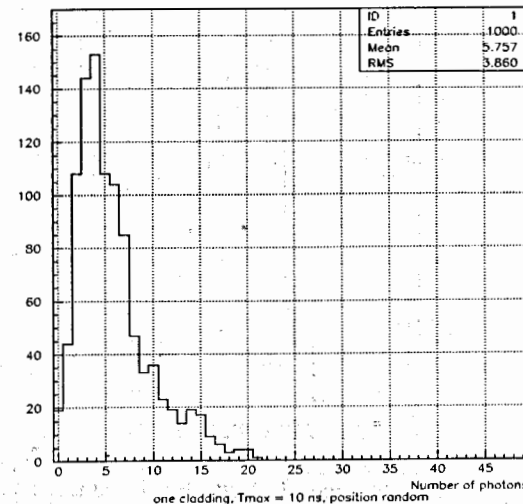


Figure 8. Distribution of the number of photons detected for conventional one cladding fiber. The average light yield is about 5.8%. The time-of-flight cut is 10 ns.

4. Summary

Our Monte Carlo calculations show that the light output of round scintillating fibers could be improved significantly by using an intercladding layer *Superfiber* design. Helical trajectories of the trapped light fraction, previously considered a deficiency of the light collection process, could then be used to enhance the light output. Medical technology would be notable beneficiary of the *superfiber* design where fiber based detectors could offer improved resolution in nuclear imaging.

An interlayered fiber design presents some challenges for fiber technology. To achieve high light yield, reflective quality of fiber surfaces must be improved by about a factor of 10. With the recent great progress in optical fiber technology, we believe that the required surface quality for the *superfiber* design is technically achievable.

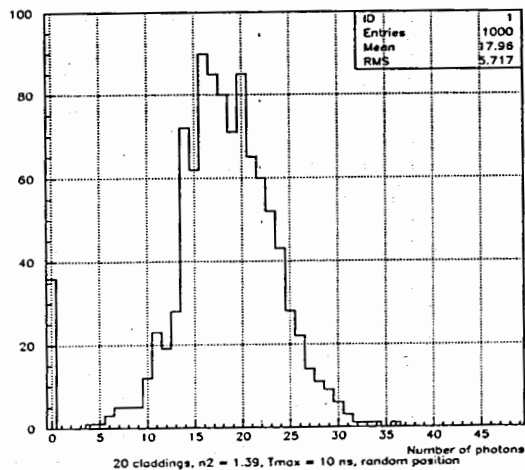


Figure 9. Light yield of about 18% is achieved for a 20-layer fiber with intercladding material having refraction index of 1.39. The time-of-flight cut is 10 ns.

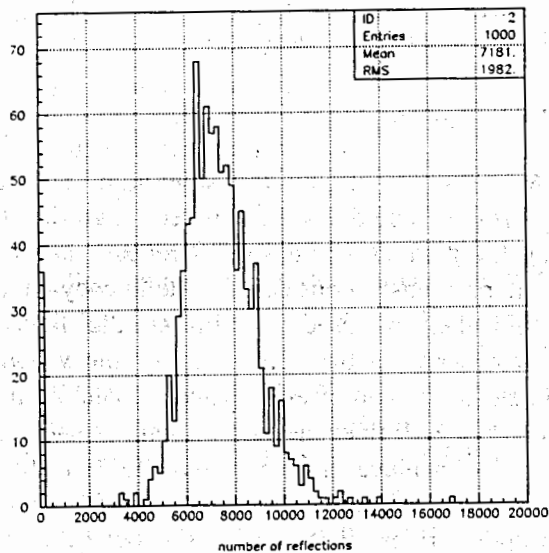


Figure 10. Distribution of events versus average number of reflections in a 20-layer fiber with cladding material of 1.39 refraction index. The time-of-flight cut is 10 ns.

Acknowledgments

The authors greatly appreciate the interest to the subject from the members of Advanced Radiological Sciences Division of the Radiology Department of the University of Texas Southwestern Medical Center. Special thanks to G. Arbique for careful reading of the manuscript.

References

1. P. V. Kulkarni, J. A. Anderson, P. P. Antich, J. O. Prior, Y. Zhang, J. Fernando, A. Constantinescu, N. C. Goomer, R. W. Parkey, E. Fenyves, R. C. Chaney, S. C. Srivastava, and L. F. Mausner, "New Approaches in Medical Imaging Using Plastic Scintillating Detectors," *Nuclear Instruments and Methods in Physics Research B79* (1993) 921-925.
2. B. Baumbaugh et al., "Performance of multicladd scintillating and clear waveguide fibers read out with visible light photon counters," *Nuclear Instruments and Methods in Physics Research A 345* (1994) 271-278.
3. P. V. Kulkarni, P. P. Antich, J. A. Anderson, J. Fernando, T. M. Aminabhavi, S. F. Harlapur, M. I. Aralagupi, and R. H. Balundgi, "Plastic scintillating materials in nuclear medical imaging", *Polymer-Plastic Technology and Engineering v. 36(1)* (1997) 1-51.
4. W. R. Binns, M. H. Israel and J. Klarmann, "Scintillator-fiber charged-particle track-imaging detector", *Nuclear Instruments and Methods 216* (1983) 475-480.
5. T. O. White, "Scintillating fibers", *Nuclear Instruments and Methods in Physics Research A273* (1988) 820-825.

Received by Publishing Department
on November 20, 1997.